International Journal of Technology (2017) 8: 1479-1488
ISSN 2086-9614

AN ANALYSIS OF THE ELECTROLYTE RESISTIVITY EFFECT ON THE PORE DIAMETER AND PORE DENSITY OF ANODIC ALUMINIUM OXIDE (AAO) FILMS PRODUCED BY SINGLE-STEP ANODIZATION

Vika Rizkia[1*], Johny Wahyuadi Soedarsono[2], Badrul Munir[2], Bambang Suharno[2]

[1]*Department of Mechanical Engineering, Politeknik Negeri Jakarta, Depok 16425, Indonesia*
[2] *Department of Metallurgy and Materials Engineering, Faculty of Engineering, Universitas Indonesia, Kampus UI Depok, Depok 16424, Indonesia*

(Received: December 2016 / Revised: May 2017 / Accepted: December 2017)

ABSTRACT

Nanoporous anodic aluminum oxide (AAO) layers were successfully fabricated on aluminum foil through an anodizing process in oxalic acid and mixed electrolytes of sulfuric and oxalic acid. The effect of electrolyte resistivity on the morphology of nanoporous AAO, such as pore diameter and pore density, was investigated. The nanoporous AAO layers'bmorphology was examined using field emission scanning electron microscopy (FE-SEM) and analyzed using image analysis software. The results showed that anodizing in mixed electrolytes (sulfuric and oxalic acid) produced a much smaller pore diameter and a much higher pore density at lower voltage compared to anodizing in a single oxalic acid. For the anodizing process in oxalic acid, the pore diameters ranged from 14 to 52 nm, and the pore density ranged from 34–106 pores in 500×500 nm^2. The anodizing process in the mixed electrolytes resulted in pore diameters within the range of 7–14 nm, and the pore densities were within the range of 211–779 pores in 500×500 nm^2. Overall, increasing the electrolyte resistivity within the same solution leads to decreased pore diameter.

Keywords: Anodic Aluminum Oxide; Electrolyte resistivity; Mixed electrolytes; Oxalic acid; Pores

1. INTRODUCTION

Nanoporous materials have received significant attention from nanotechnologists and material scientists in recent years due to their unique and attractive properties (Prihandana et al., 2015; Dhaneswara & Sofyan, 2016). Compared to the conventional lithographic techniques, anodizing is a cheaper, simpler, and less time-consuming method for nanoporous material fabrication in aluminum. Therefore, today, anodizing has been widely adopted in the industry (Bensalah et al., 2011; Keshavarz et al., 2013). Anodizing can produce a self-organizing and homogeneous morphology of porous anodic aluminum oxide (AAO) with peculiar characteristics, such as a large surface to volume ratio, a dielectric constant, good adhesion, mechanical strength, thermal stability, and corrosion resistance (Kao & Chang, 2014; Lee et al., 2013; Keshavarz et al., 2013). Porous AAO has been applied as nano-templates and resistance films for magnetic and photonic devices (Nguyen et al., 2017; Chung et al., 2017) , biosensors (Wu et al., 2015), biotechnology (Kang et al., 2007; Ingham et al., 2012), or surface-enhanced Raman scattering (Hao et al., 2012).

Since Keller et al. introduced the first classical model for AAO in 1953 (Voon et al., 2013),

*Corresponding author's email: vee_mt03@yahoo.com, Tel: +62-21-7863510, Fax: +62-21-7872350
Permalink/DOI: https://doi.org/10.14716/ijtech.v8i8.742

many researchers have worked on the porous AAO phenomenon on aluminum and its alloys. They have reported porous AAO formed on anodized aluminum with pore diameters in the range of 13–273 nm and pore densities of 10^{13} pores/cm^2 (Bartolomé et al., 2006; Gao et al., 2008; Tamburrano et al., 2011).

The mechanism of porous AAO formation is still debated; previous reports have attributed it to the dynamic equilibrium of aluminum oxide formation and local field-assisted aluminum oxide dissolution (barrier layer dissolution; Vrublevsky et al., 2006; Sulka, 2008; Chung et al., 2011; Kikuchi et al., 2014). Many studies have shown that porous AAO morphology, such as pore diameter, pore wall thickness, porosity, interpore distance, and pore density, can be controlled simply by varying the anodizing parameters (Sulka & Parkoła 2007; Belwalkar et al., 2008; Chung et al., 2011; Tamburrano et al., 2011; Theohari & Kontogeorgou, 2013; Zaraska et al. 2013). Temperature plays an important role during the anodizing process and significantly affects the morphology of porous AAO (Sulka & Parkoła, 2007; Theohari & Kontogeorgou, 2013). Our previous study showed that an appropriate anodizing temperature produced a porous morphology with good adhesion properties for further coating (Rizkia et al., 2014; Rizkia et al., 2015). Higher anodizing temperature resulted in higher current density and the chemical dissolution of the oxide surface, resulting in porous AAO with wider pores and thinner pore walls (Sulka & Parkoła, 2007; Zahariev et al. 2008; Aerts et al., 2009; Aerts et al., 2010 Zaraska et al., 2013; Kao & Chang, 2014). Beside temperature, anodizing voltage is also an important parameter that significantly influences porous AAO features (Vrublevsky et al., 2012). Increasing anodizing voltage results in increasing volume expansion factors until the vertex drops significantly (Kao & Chang, 2014). In addition, increasing anodizing voltage yields porous AAO with regularly arranged pores and larger pore diameters. This phenomenon occurs due to the increasing of the electric field's strength, the ion transport number, and the electron conductivity within the AAO and the dissolution of AAO at the oxide/electrolyte interface (Wang et al., 2006; Sulka & Parkoła, 2007; Stêpniowski et al., 2012). The first step of anodizing also plays an important role during aluminum oxide formation, as the first oxide formed serves as a pre-texturation for the aluminum beneath the pore bottom. Longer anodizing times result in stronger pre-texturation and a better arrangement of the AAO nanoporous array (Stepniowski et al., 2011).

In respect to the type of electrolyte, Wang et al. (2006) reported that increasing the sulfuric acid concentration leads to increasing the current density due to the high solubility of the AAO. Keshavarz et al. (2013) also showed that AAO pore diameters produced by anodizing in sulfuric acid are smaller than those anodized in oxalic acid and a mixture of sulfuric and oxalic acids. The AAO nanopore regularity produced by anodizing in oxalic acid is much lower due to the significantly slower oxide growth rate than that of single sulfuric acid or mixed acids. Therefore, electrolyte resistivity could become a critical factor that might affect the morphology of porous AAO. Yet, the studies of electrolyte solution resistivity in accordance with the anodizing process are extremely limited. Thus, the current paper reports and discusses the influence of electrolyte solution resistivity on porous AAO morphology (pore diameter and density).

2. EXPERIMENTAL

2.1. Pretreatment and Anodic Oxidation of Aluminum Foil by a Single-step Anodizing Process

Kiln Pack commercial aluminum foil (98.2% Al), with a thickness of approximately 20 microns, was selected as a specimen. A one-sided 25×25 mm^2 surface area of the specimen was prepared and exposed to electrolytes. Prior to anodizing, to remove the natural oxide layer and grease, the specimens were degreased in 60 g/l NaOH solution at 60–70^{o}C until bubbles

appeared on the surface of the specimens. Subsequently, the specimens were rinsed thoroughly in water and acetone. The fabrication of porous AAO was conducted by a single-step anodizing process in single $H_2C_2O_4$ (pa. grade Merck) solution and a mixed-electrolyte solution of $H_2C_2O_4$ and H_2SO_4 (pa. grade Mallinckrodt). A carbon bar was used as the cathode. Anodizing was performed under potentiostatic conditions applied by using a Protek DC Power Supply. Table 1 shows the experimental parameters applied in this research.

Table 1 The experimental anodizing parameters used in this research

No.	Electrolyte	Anodizing Parameters
1	0.3 M $H_2C_2O_4$	
2	0.4 M $H_2C_2O_4$	V = 45 V
3	0.5 M $H_2C_2O_4$	T = Room temp
4	0.6 M $H_2C_2O_4$	t = 40 and 50 minutes
5	0.7 M $H_2C_2O_4$	
6	3 M H_2SO_4 + 0.5 M $H_2C_2O_4$	V = 15 V, T = 30^{o}C, t = 40 and 50 minutes

2.2. Calculation of Electrolyte Resistivity

Electrolyte solution resistance was examined using a Ground Resistance Tester, model 4610, AEMC Instrument in a Miller Soil Box electrode with the cross-section (A) and separation length (L) of 12.8 cm^2 and 22.2 cm, respectively. From the measured resistance, the electrolyte resistivity was obtained from the second Ohm's law equation (Benenson et al., 2002):

$$\rho = \mathbf{R}.\mathbf{A}/\boldsymbol{L} \quad (1)$$

where ρ is electrolyte resistivity (Ω.cm), R is measured electrolyte resistance (Ω), A is a cross-sectional area of each electrode (cm^2), and L is the gap separating the electrodes (cm).

2.3. Porous AAO Characterization

Characterizing the surface morphology of the porous AAO was performed using field emission scanning electron microscopy (FE-SEM, FEI Inspect F50). Prior to the FE-SEM characterization, as-anodized aluminum foil specimens were gold-sputtered for observing higher resolutions. The pore diameters and pore densities obtained from the FE-SEM were analyzed using Image Pro Analysis version 7.0 software. Furthermore, pore density was estimated using the "manual tag" pore count in Image Pro Analysis 7.0 software. Pore density is determined as a ratio of the number of pores to a selected area (500×500 nm^2; Belwalkar et al., 2008; Chung et al., 2011).

3. RESULTS AND DISCUSSION

3.1. Effects of Oxalic Acid Electrolyte Resistivity on Porous AAO Surface Morphology

Figure 1 depicts the typical FE-SEM images of the surface morphology of AAO pores produced by the anodizing process in 0.3, 0.5, and 0.7 M $H_2C_2O_4$ solution at 45 V for 40 minutes at room temperature. The AAO pores' morphology shows a random pattern but a uniform distribution. This result is in agreement with the findings of Bensalah et al. (2011). Different pore diameters and densities are revealed for different oxalic acid concentrations and times. The higher the oxalic acid concentration, the wider the pore diameter. The AAO pores produced by anodizing in 0.3 M oxalic acid were incipient pores, which transformed into true pores with the increasing of oxalic acid concentration. Furthermore, the AAO pores produced by anodizing in a single oxalic acid solution had the average diameter range of 14.3±2.3 to 52.9±9.4 nm, with pore densities ranging from 34.0±1.2 to 106±2.4 pores per 500×500 nm^2 (all AAO pores obtained were assumed to be perfectly circular in shape).

Table 2 tabulates the data of pore diameter and density with respect to oxalic acid concentration and anodizing time. As shown in Table 2, when the oxalic acid concentration increased from 0.3 to 0.7 M, the electrolyte resistivity decreased from 16.09 to 10.13 Ω-cm. Resistivity is a reciprocal function of conductivity. Electrolyte conductivity is the ability of an electrolyte to conduct electricity through the motion of charged particles (ions within an electrolyte). The main factors that strongly affect ionic conductivity in electrolytes are the concentration of free charge carriers (ions) and the ability of the charge carriers (ions) to move in an electric field (Gering, 2017). With an increase in the oxalic acid concentration, the concentration of dissolved salt in an electrolyte phase and the ionic mobility are increased, which results in higher electrolyte conductivity and lower resistivity. Furthermore, this decreased resistivity affects pore diameter, as shown in Figure 1.

Table 2 Measured electrolyte resistivity and the morphology of AAO pores produced by anodizing in a single oxalic acid

M	ρ (Ω.cm)	40 minutes		50 minutes	
		Diameter	Density	Diameter	Density
0.7	10.13	49.8±6.6	36.4±1.8	52.9±5.5	34±1.2
0.6	12.63	48.4±6.5	38.6±0.6	49.4±6.6	31.8±2.5
0.5	12.74	39.0±3.3	44.1±1.2	46.1±5.0	36±0.4
0.4	15.39	27.1±3.5	49.5±2.2	27.9±4.0	35.4±2.5
0.3	16.09	14.3 ±2.3	106±2.4	19.4 ±2.5	62.8±1.8

*Diameter (nm), density (pores/500×500 nm^2)

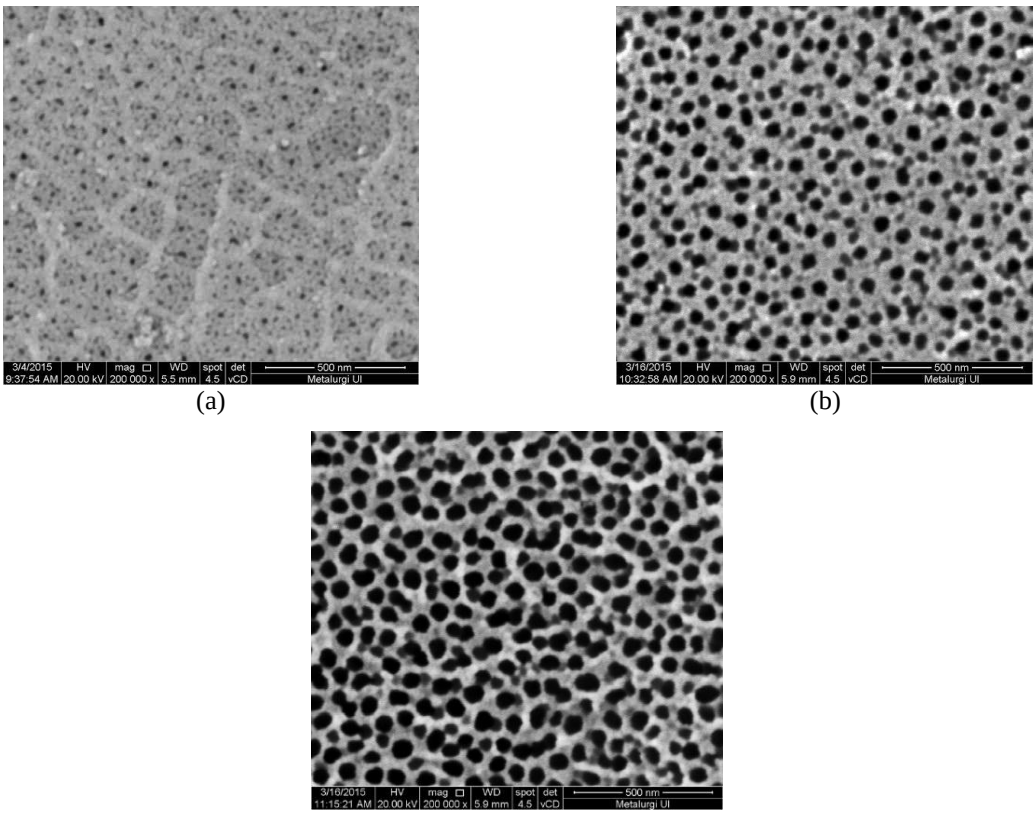

(a) (b)

(c)

Figure 1 FE-SEM micrograph of AAO pores produced by single-step anodizing in: (a) 0.3 M; (b) 0.5 M; and (c) 0.7 M $H_2C_2O_4$ electrolyte solution at room temperature

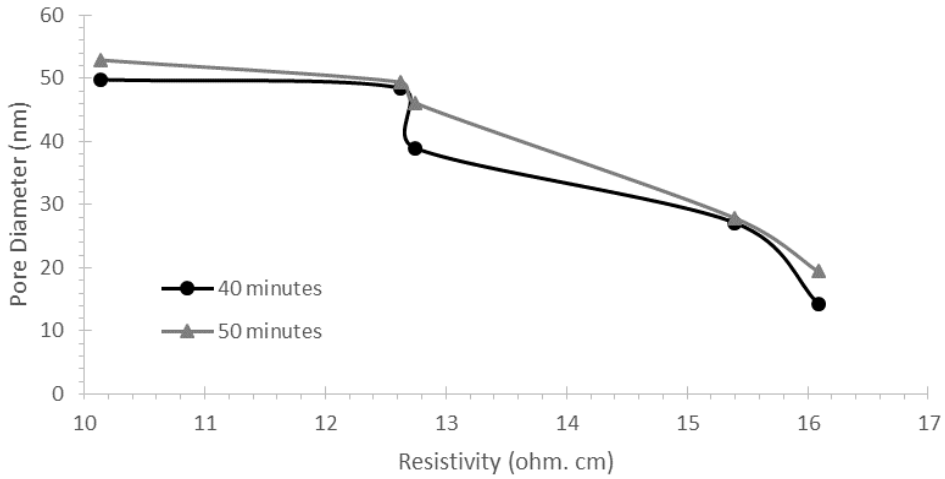

Figure 2 The relationship between the pore diameters and oxalic acid electrolyte resistivity

Diffusion is the most common mechanism in liquid solutions; hence, the ions' diffusion coefficient during anodizing might greatly affect the formation of AAO pores. Based on Einstein's equation, diffusion coefficient (D) is linearly dependent on the ionic mobility, which is the ability of free ions to move in an electric field (Stępniowski et al., 2014):

$$\boldsymbol{D = kTu|z|} \tag{2}$$

As shown in Table 2, the higher the oxalic acid concentration, the higher the ionic mobility and the lower the electrolyte resistivity. Thus, the diffusion coefficient increases according to Equation 2. Therefore, it is expected that the oxygen and hydroxide ions' availability and the aluminum ions' release should be increased. A higher oxide dissolution rate and the formation of wider pores may occur. Furthermore, increased ionic mobility is believed to cause increased current density, which provides a higher stimulant for the increased local temperature. The increased ionic mobility also resulted in a higher oxide dissolution rate in the aluminum/oxide interface and in wider pores.

Regarding the electrolyte resistivity effect on other porous morphology, Figure 3 shows a relationship between the AAO pore density and the electrolyte resistivity produced by anodizing in a single oxalic acid electrolyte. With increasing electrolyte resistivity, an increase in pore density occurs. This phenomenon is possibly attributed to the decreasing pore diameter and the increasing electrolyte resistivity.

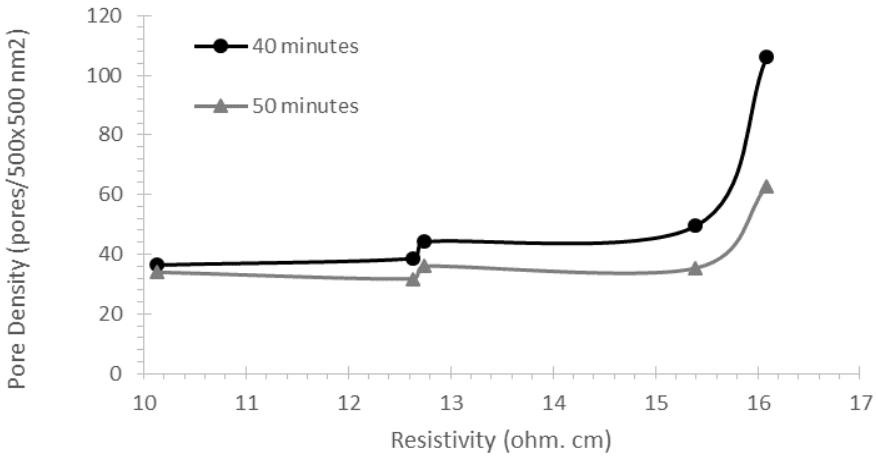

Figure 3 The relationship between pore densities and oxalic acid electrolyte resistivity

An increase in pore diameter leads to a decrease in the density of the pores formed on the aluminum surface. This behavior was related to the merging of adjacent pores due to the enhancement of chemical dissolution in lower electrolyte resistivity. This obtained result agrees with Sulka's (2008) findings. The research presumes that the decreased pore density was found with increased pore diameter, and this behavior was attributed to the rearrangement of pores due to the transformation of initial pores into true pores.

3.2. Effect of Adding 3 M Sulfuric Acid to Oxalic Acid Electrolytes on AAO Pore Morphology

Figure 4 shows the typical FE-SEM images of the surface morphology of AAO pore films produced by anodizing in mixed electrolytes of 3 M H_2SO_4 and 0.5 and 0.7 M $H_2C_2O_4$ solution with a DC voltage of 15 V applied for 40 minutes at 30^oC. The AAO pores were successfully fabricated by anodizing in the mixed electrolytes. The AAO pores produced were extremely tiny; therefore, the pore densities were very high. According to Figures 1 and 4, in general, the addition of sulfuric acid into oxalic acid provides much smaller pore diameters and much higher pore densities at lower voltages (15 V) than that of single oxalic acid during the anodizing process. In this research, the formation of pores as small as 7 nm in diameter was produced by adding 3 M sulfuric acid into oxalic acid, while the pore densities obtained were 779.3±17.5 in 500×500 nm^2.

Table 3 summarizes the data of pore morphology (pore diameter and pore densities) with respect to the addition of 3 M sulfuric acid into oxalic acid electrolyte. Table 3 indicates that compared to the anodizing process in single oxalic acid (Table 2), the addition of 3 M sulfuric acid into oxalic acid resulted in much lower electrolyte resistivity. For instance, the electrolyte resistivity of 0.5 M oxalic acid decreased significantly from 12.8 to 2.1 Ω.cm after the addition of 3 M sulfuric acid. From Figure 5 and Table 3, one can infer that when 3 M sulfuric acid has been added into oxalic acid, the electrolyte resistivity will be drastically decreased, leading to decreased pore diameter and significantly increased pore density.

The formation of pores as small as 7 nm in diameter and a highly significant difference in pore morphology between the two types of electrolyte solutions during anodizing can be explained by the influence of the electrolyte acidity. In fact, sulfuric acid is a strong acid that is fully dissociated in solution, while oxalic acid is a weak acid that is partially dissociated in solution. Thus, once a strong acid (sulfuric acid) is added to a weak acid (oxalic acid), the dissociated ions within the electrolyte solution greatly increase. Consequently, ionic mobility becomes much higher and generates a significant decrease in electrolyte resistivity. The diffusion coefficient could also be increased drastically, as expressed in equation (2), and this leads to the increased supply of oxygen and hydroxide ions and the release of aluminum ions. Therefore, a higher oxide dissolution rate and increased pore nucleation may occur. Consequently, smaller pore diameters and higher pore densities were observed.

Table 3 Measured electrolyte resistivity and the morphology of AAO pores produced by anodizing in mixed electrolytes

M	ρ (Ω.cm)	40 minutes		50 minutes	
		Diameter	Density	Diameter	Density
3 M H_2SO_4 + 0,5 M $H_2C_2O_4$	2.12	9.4±1.2	566.5±34.0	14.6±3.9	428.4±5.9
3 M H_2SO_4 + 0,7 M $H_2C_2O_4$	2.4	7.2±1.2	779.25±17.5	8.3±1.6	211.6±5.8

*Diameter (nm), density (pores per 500×500 nm^2)

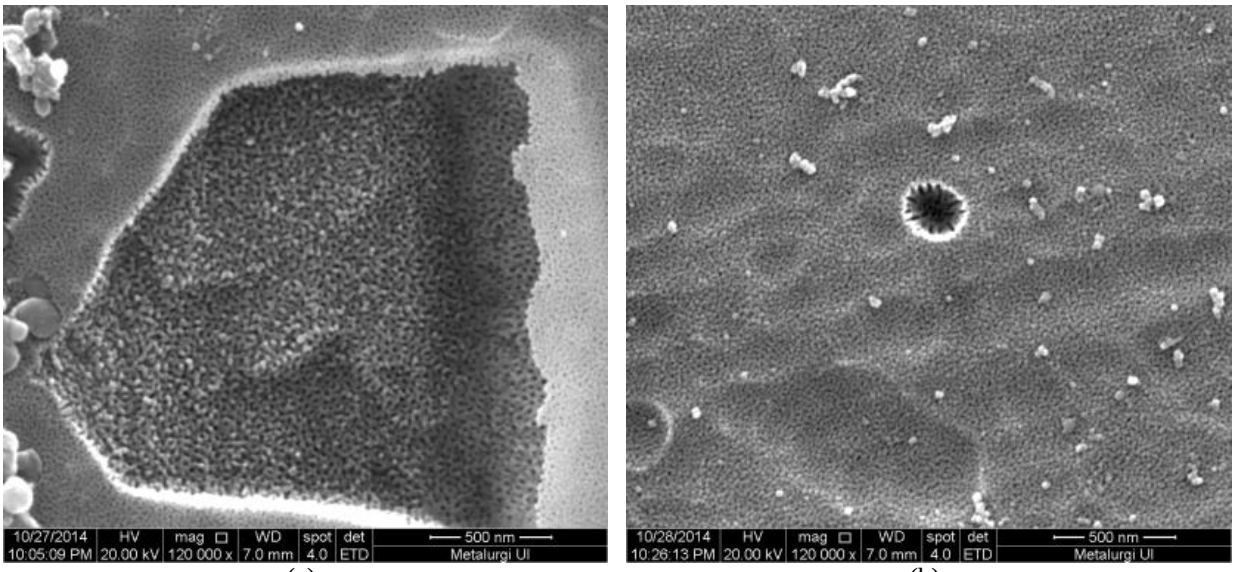

(a) (b)

Figure 4 FE-SEM micrograph of AAO pores produced by single-step anodizing in mixed electrolytes of 3 M H_2SO_4 and: (a) 0.5 M; and (b) 0.7 M $H_2C_2O_4$

Figure 5 illustrates the influence of electrolyte resistivity on the pore diameter obtained during anodizing in all the studied electrolytes. As discussed previously in Figure 2, the pore diameter produced by anodizing in a single oxalic acid has a linear relationship with electrolyte resistivity; the pore diameter increases with the decreasing of electrolyte resistivity. Yet, if all the data (pore diameter produced by anodizing in single oxalic acid and mixed electrolytes) were combined, the result shows a scalloped curve; thus, the linear relationship does not exist. For instance, as seen in Figure 5, anodizing in an electrolyte with the resistivity of approximately 2 Ω-cm produced a much smaller pore diameter, while anodizing at the resistivity of 10 Ω-cm produced a significant increase in pore diameter. Later, a slow drop in pore diameter was noted when increasing the electrolyte resistivity up to 16 Ω-cm. This phenomenon indicates the increasing electrolyte resistivity leads to decreasing the pore diameter only in the same type of electrolyte solution.

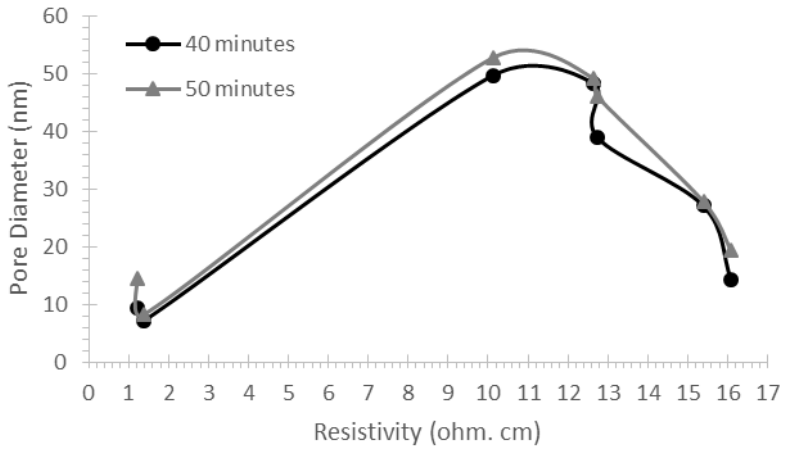

Figure 5 The relationship between the pore diameter and electrolyte resistivity for all the studied electrolytes

4. CONCLUSION

Nanoporous AAO was successfully fabricated on aluminum foil through an anodizing process in oxalic acid and a mixed electrolyte of sulfuric and oxalic acids. Generally, the type of electrolyte and its resistivity can control pore diameter and density. For the anodizing process in oxalic acid, the measured pore diameter was in the range of 14.3±2.3 to 52.9±5.5 nm, and the pore density was in the range of 34±1.2 to 106±2.4 pores in 500×500 nm^2. The higher the oxalic acid concentration, the wider the pore diameter and the lower the pore density produced. Adding 3 M sulfuric acid to oxalic acid electrolyte produced much smaller pore diameters and much higher pore densities at lower voltage compared to anodizing in a single oxalic acid. This mixed electrolyte produced a pore morphology as small as 7.2±1.2 nm in diameter and a density of 779.3±17.5 pores per 500×500 nm^2. The significant difference in the diameter was attributed to the electrolyte's acidity, which affects the electrolyte's resistivity. Increasing the electrolyte resistivity within the same type of solution led to decreasing the pore diameter.

5. REFERENCES

Aerts, T., De Graeve, I., Terryn, H., 2009. Control of the Electrode Temperature for Electrochemical Studies: A New Approach Illustrated on Porous Anodizing of Aluminium. *Electrochemistry Communications*, Volume 11(12), pp. 2292–2295

Aerts, T., Jorcin, J.-B., Graeve, I.D., Terryn, H., 2010. Comparison between the Influence of Applied Electrode and Electrolyte Temperatures on Porous Anodizing of Aluminium. *Electrochimica Acta*, Volume 55(12), pp. 3957–3965

Bartolomé, M.J., Lopez, V., Escudero, E., Caruana, G., Gonzales, J.A., 2006. Changes in the Specific Surface Area of Porous Aluminium Oxide Films during Sealing. *Surface and Coatings Technology*, Volume 200(14–15), pp. 4530–4537

Belwalkar, A., Grasing, E., Geertruyden,W.V., Huang, Z., Misiolek, W.Z., 2008. Effect of Processing Parameters on Pore Structure and Thickness of Anodic Aluminum Oxide (AAO) Tubular Membranes. *Journal of Membrane Science*, Volume 319(1–2), pp. 192–198

Benenson, W., Harris, J.W., Stocker, H., Lutz, H., 2002. *Handbook of Physics* (1st ed.). New York, NY: Springer-Verlag New York

Bensalah, W., Feki, M., Wery, M., Ayedi, H.F., 2011. Chemical Dissolution Resistance of Anodic Oxide Layers Formed on Aluminum. *Transactions of Nonferrous Metals Society of China (English Edition)*, Volume 21(7), pp. 1673–1679

Chung, C.K., Liao, M.W., Chang, H.C., Lee, C.T., 2011. Effects of Temperature and Voltage Mode on Nanoporous Anodic Aluminum Oxide Films by One-step Anodization. *Thin Solid Films*, Volume 520(5), pp. 1554–1558

Chung, C.K., Li, C.H., Hsieh, Y.Y., Wang, Z.W., 2017. Microstructure and Photoluminescence of Sputtered Silicon-rich-nitride on Anodic Aluminum Oxide Annealed at Low Temperature. *Journal of Alloys and Compounds*, Volume 709, pp. 658–662

Dhaneswara, D., Sofyan, E., 2016. Effect of Different Pluronic P123 Triblock Copolymer Surfactant Concentrations on SBA-15 Pore Formation. *International Journal of Technology*, Volume 7(6), pp. 1009–1015

Gao, L., Wang, P., Wu, X., Yang, S., Song, X., 2008. A New Method Detaching Porous Anodic Alumina Films from Aluminum Substrates. *Journal of Electroceramics*, Volume 21(1–4), pp. 791–794

Gering, K.L., 2017. Prediction of Electrolyte Conductivity: Results from a Generalized Molecular Model based on Ion Solvation and a Chemical Physics Framework. *Electrochimica Acta*, No. 225, pp. 175–189

Hao, Q., Qiu, T., Chu, P.K., 2012. Surfaced-enhanced Cellular Fluorescence Imaging. *Progress*

in Surface Science, Volume 87(1–4), pp. 23–45

Ingham, C.J., ter Maat, J., de Vos, W.M., 2012. Where Bio Meets Nano: The Many Uses for Nanoporous Aluminum Oxide in Biotechnology. *Biotechnology Advances*, Volume 30(5), pp. 1089–1099

Kang, H.-J., Kim, D.J., Park, S.-J., Yoo, J.-B., Ryu, Y.S., 2007. Controlled Drug Release Using Nanoporous Anodic Aluminum Oxide on Stent. *Thin Solid Films*, Volume 515(12), pp. 5184–5187

Kao, T.T., Chang, Y.C., 2014. Influence of Anodization Parameters on the Volume Expansion of Anodic Aluminum Oxide Formed in Mixed Solution of Phosphoric and Oxalic Acids. *Applied Surface Science*, Volume 288, pp. 654–659

Keshavarz, A., Parang, Z., Nasseri, A., 2013. The Effect of Sulfuric Acid, Oxalic Acid, and Their Combination on the Size and Regularity of the Porous Alumina by Anodization. *Journal of Nanostructure in Chemistry*, Volume 3(34), https://doi.org/10.1186/2193-8865-3-34

Kikuchi, T., Yamamoto, T., Natsui, S., Suzuki, R.O., 2014. Fabrication of Anodic Porous Alumina by Squaric Acid Anodizing. *Electrochimica Acta*, No. 123, pp. 14–22

Lee, J., Jung, U., Kim, W., Chung, W., 2013. Effects of Residual Water in the Pores of Aluminum Anodic Oxide Layers Prior to Sealing on Corrosion Resistance. *Applied Surface Science*, Volume 283, pp. 941–946

Prihandana, G.S., Sriani, T., Mahardika, M., 2015. Review of Surface Modification of Nanoporous Polyethersulfone Membrane as a Dialysis Membrane. *International Journal of Technology*, Volume 6(6), pp. 1025–1030

Nguyen, V.H., Sichanugrist, P.,Kato, S., Usami, N., 2017. Impact of Anodic Aluminum Oxide Fabrication and Post-deposition Anneal on the Effective Carrier Lifetime of Vertical Silicon Nanowires. *Solar Energy Materials and Solar Cells*, Volume 166, pp. 39–44

Rizkia, V., Munir, B., Soedarsono, J.W., Suharno, B., Rustandi, A., 2014. Growth of Porous Alumina Layer and Cerium Sealing of Al7xxx/SiC Composite for Structural Lightweight Alloy Corrosion Resistant Application. *Advanced Materials Research*, Volume 911, pp. 55–59

Rizkia, V., Munir, B., Soedarsono, J.W., Suharno, B., 2015. Corrosion Resistance Enhancement of an Anodic Layer on an Aluminum Matrix Composite by Cerium Sealing. *International Journal of Technology*, Volume 6(7), pp. 1191–1197

Stêpniowski, W.J., Norek, M., Michalska-Domanska, M., Bombalska, A., Nowak-Stepniowska, A., Kwasny, M., Bojar, Z., 2012. Fabrication of Anodic Aluminum Oxide with Incorporated Chromate Ions. *Applied Surface Science*, Volume 259, pp. 324–330

Stępniowski, W.J., Forbot, D., Norek, M., Michalska-Domanska, M., Krol, A., 2014. The Impact of Viscosity of the Electrolyte on the Formation of Nanoporous Anodic Aluminum Oxide. *Electrochimica Acta*, Volume 133, pp. 57–64

Stepniowski, W.J., Zasada, D., Bojar, Z., 2011. First Step of Anodization Influences the Final Nanopore Arrangement in Anodized Alumina. *Surface & Coatings Technologys*, Volume 206, pp. 1416–1422

Sulka, G.D., 2008. *Highly Ordered Anodic Porous Alumina Formation by Self Organized Anodizing* A. Eftekhari, ed., Weinheim: Wiley-VCH Verlag GmbH & Co

Sulka, G.D., Parkoła, K.G., 2007. Temperature Influence on Well-ordered Nanopore Structures Grown by Anodization of Aluminium in Sulphuric Acid. *Electrochimica Acta*, Volume 52(5), pp. 1880–1888

Tamburrano, A., Vivo, B.D., Hoijer, M., Arurault, L., Tucci, V., Fontorbes, S., Lamberti, P., Vilar, V., Daffos, B., Sarto, M.S., 2011. Effect of Electric Field Polarization and Temperature on the Effective Permittivity and Conductivity of Porous Anodic Aluminium Oxide Membranes. *Microelectronic Engineering*, Volume 88(11), pp. 3338–3346

Theohari, S., Kontogeorgou, C., 2013. Effect of Temperature on the Anodizing Process of Aluminum Alloy AA 5052. *Applied Surface Science*, Volume 284, pp. 611–618

Voon, C.H., Derman, M.N., Hashim, U., Ahmad, K.R., Foo, K.L., 2013. Effect of Temperature of Oxalic Acid on the Fabrication of Porous Anodic Alumina from Al-Mn Alloys. *Journal of Nanomaterials*, Volume 2013, pp. 1–8

Vrublevsky, I., Parkoun, V., Schreckenbach, J., Goedel, W.A., 2006. Dissolution Behaviour of the Barrier Layer of Porous Oxide Films on Aluminum Formed in Phosphoric Acid Studied by a Re-anodizing Technique. *Applied Surface Science*, Volume 252(14), pp. 5100–5108

Vrublevsky, I., Chernyakova, K., Bund, A., Ispas, A., Schmidt, U., 2012. Effect of Anodizing Voltage on the Sorption of Water Molecules on Porous Alumina. *Applied Surface Science*, Volume 258(14), pp. 5394–5398

Wang, Y., Kuo, H.H., Kia, S., 2006. Effect of Alloy Types on the Anodizing Process of Aluminum. *Surface & Coatings Technology*, Volume 200, pp. 2634–2641

Wu, C., Sun, H., Li, Y., Liu, X., Du, X., Wang, X., Xu, P., 2015. Biosensor based on Glucose Oxidase-nanoporous Gold Co-catalysis for Glucose Detection. *Biosensors and Bioelectronics*, Volume 66, pp. 350–355

Zahariev, A., Kanazirski, I., Girginov, A., 2008. Anodic Alumina Films Formed in Sulfamic Acid Solution. *Inorganica Chimica Acta*, Volume 361(6), pp. 1789–1792

Zaraska, L., Stepniowski, W.J., Ciepiela, E., Sulka, G.D., 2013. The Effect of Anodizing Temperature on Structural Features and Hexagonal Arrangement of Nanopores in Alumina Synthesized by Two-step Anodizing in Oxalic Acid. *Thin Solid Films*, Volume 534, pp. 155–161